*Transactions of the Korean Nuclear Society Autumn Meeting*
*Changwon, Korea, October 24-25, 2024*

# Core Design Study for Soluble Boron-Free and Long-cycle Operation of Small Modular Reactor using Enriched Gadolinia

Chanwoo Kim[a], Kyeongwon Kim[a], Jinsu Park[a], Eun Jeong[a], Deokjung Lee[a*]
[a]*Department of Nuclear Engineering, Ulsan National Institute of Science and Technology,*
*50 UNIST-gil, Eonyang-eup, Ulju-gun, Ulsan 44919, Republic of Korea*
[*]*Corresponding author: deokjung@unist.ac.kr*

***Keywords : SMR, Soluble Boron-Free, long-cycle operation, enriched gadolinia, STREAM/RAST-K**

## 1. Introduction

In response to global climate change, there is a growing demand for the development of small modular reactors (SMRs) due to their superior safety and flexibility compared to large commercial reactors as part of the efforts toward carbon neutrality. The need to enhance core safety in SMRs has driven the emergence of soluble boron-free (SBF) operation.

Reactor design is simplified and boron-related issues are resolved by eliminating the chemical and volume control system (CVCS), and inherent safety is improved by the absence of boron with a strongly negative moderator temperature coefficient. However, burnable absorbers and control rods have to take on the roles that boron once performed. In contrast to boron, burnable absorbers and control rods cannot be employed consistently, which results in greater power peaks, smaller operating margins, and changes in local power distribution. The increasing reliance on control rods to manage excessive reactivity may negatively impact reactor operability and safety. Burnable absorbers are currently playing a critical part in SBF operation.

Recently, burnable absorbers such as centrally shielded burnable absorber (CSBA) and cylindrically inserted and mechanically separated burnable absorber (CIMBA) have been developed to enhance the self-shielding effect, thereby delaying the complete burnout point of the burnable absorber [1]. Additionally, highly intensive and discrete gadolinia/alumina burnable absorber (HIGA), which encases $Gd_2O_3$ in $Al_2O_3$, has also been developed to overcome thermal property issues associated with increased gadolinia content [2]. Although multiple burnable absorbers have been developed, manufacturing challenges still exist, and developing new burnable absorbers requires extensive testing as well as regulatory approval for unconventional fuel types.

This study aims to evaluate the feasibility and effectiveness of using enriched gadolinia to achieve SBF and long-cycle operation without relying on newly developed burnable absorbers. Gadolinia was selected for this study due to its large thermal neutron absorption cross-section and its sufficiently high melting point (2,693 K). However, gadolinia has the disadvantage that when combined with $UO_2$, its thermal conductivity decreases as its amount increases, leading to deteriorated thermal properties. Enriched gadolinia can potentially improve thermal conductivity and effectively control excess reactivity by allowing for a reduction in gadolinia content [3].

## 2. Core Design

Compared to other isotopes, $^{155}Gd$ and $^{157}Gd$ have much larger neutron absorption cross sections, which is why these two isotopes have been selected for enrichment. The difference in multiplication factors between fuel enriched with $^{155}Gd$, $^{157}Gd$, and a mixture of both isotopes is less than 1%, indicating that their effects are very similar [3]. Therefore, this study used equal proportions of both isotopes for enrichment.

Due to limitations in thermal properties, gadolinia is used at a content of 6 to 8 wt.% in commercial reactors. To enable long-cycle operation, different enrichment levels were tested using the maximum gadolinia content of 8 wt.% employed in commercial reactors. Fig. 1 shows that as gadolinia enrichment increases, the point of complete gadolinia burnout shifts towards the end of cycle (EOC).

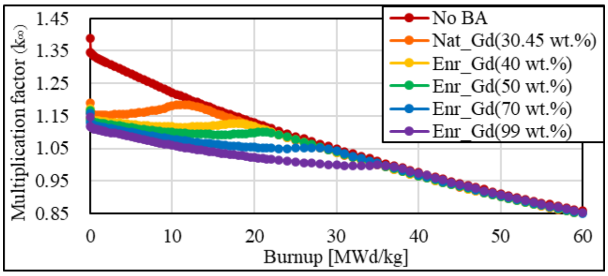


Fig. 1. Comparison of $k_\infty$ for various gadolinia enrichment

Using only enriched gadolinia makes it challenging to control high excess reactivity at the beginning of cycle (BOC). To manage this issue, a fuel mix of enriched gadolinia and low-content natural gadolinia was employed. This approach benefits from the rapid burnout of the low-content natural gadolinia to better control excess reactivity at BOC [4]. Using a gadolinia content of 8 wt.%, fuel with a flat reactivity curve was achieved by adjusting the number of gadolinia pins and the $^{235}U$ enrichment for each enrichment level of $^{155,157}Gd$. The content of natural gadolinia was then varied from 0.3 to 4 wt.% and mixed with enriched gadolinia, resulting in the identification of an optimized fuel with a flat reactivity curve. $UO_2$ sintered pellet was mixed with enriched gadolinia of the same enrichment level and low-content natural gadolinia. Fig. 2 illustrates the variation in the multiplication factor with changes in the low-content natural gadolinia. It shows that as the content of natural gadolinia increases, the multiplication factor at BOC decreases.

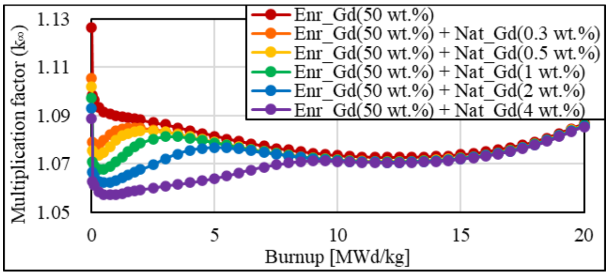


Fig. 2. Comparison of $k_\infty$ for various natural gadolinia contents

*2.1 Computation Code System*

The core design and analysis were performed using the two-step codes STREAM and RAST-K. STREAM conducts lattice physics calculations for generating group constants for core calculations by solving the neutron transport equation using the method of characteristics [5]. RAST-K is a nodal code based on a 3D multi-group unified nodal method with multi-group coarse mesh finite difference acceleration [5].

*2.2 Fuel Assembly Design*

The design parameters and design limits of the reactor utilizing enriched gadolinia for reactivity control are summarized in Table I. The shutdown margin limit was determined based on the mPower reactor, one of the SBF SMRs with similar geometries (17 × 17 square-type assemblies), uranium enrichment (< 5 wt.%), and an active core height of 2 m [6].

Table I: Design parameter

| Parameter | Value |
|---|---|
| Thermal power [$MW_{th}$] | 520 |
| Number of FAs | 69 |
| Fuel enrichment [wt.% $^{235}U$] | < 4.95 |
| Control rod material | AIC |
| Reflector material | Stainless steel |
| Active core height [m] | 2.4 |
| Total loading [MTU] | 21.613 |
| Multiplication factor ($k_{eff}$) | 1.005 < $k_{eff}$ < 1.015 |
| 3D pin peaking factor ($F_q$) | $F_q$ < 2.5 |
| Axial Shape Index (ASI) | -0.4 < ASI < +0.4 |
| Isothermal temperature coefficient | ITC < 0 pcm/°C |
| Shutdown margin | SDM > 3000 pcm |
| Target cycle length | ~30 months |

When control rods are used to regulate excess reactivity in a reactor, power tends to concentrate at the bottom of the core, leading to a higher ASI value and increased axial asymmetry. To minimize the use of control rods, the strategy focused on managing excess reactivity as much as possible using burnable absorbers. Fuel was selected based on the criterion that the difference between the maximum and minimum multiplication factor remained within approximately 5,000 pcm throughout the fuel burnup. Fig. 3 shows 2D fuel assembly configurations for core calculations.

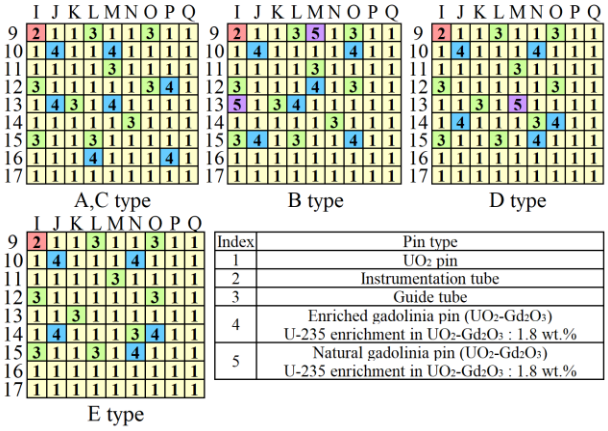


Fig. 3. Quarter pin patterns of 2D fuel assembly

The axial configuration of the core was designed homogeneously to simplify fuel manufacturing. Table II provides details on the types of fuel used in the core, and Fig. 4 shows both the loading and control rod patterns. In region A of Fig. 4, fuel with multiplication factor less than unity was used to prevent power peaking at the core's center. Conversely, in regions D and E, located at the periphery of the core, fuel with relatively higher $^{235}U$ enrichment was used to compensate for the lower multiplication factor in the center.

Table II: Compositions of fuel assembly types

| Fuel type | A | B | C | D | E |
|---|---|---|---|---|---|
| $^{235}U$ enrichment [wt.%] | 4 | 4 | 4 | 4.5 | 4.95 |
| Number of gadolinia pin (Enr + Nat) | 28 | 24 + 4 | 28 | 20 + 4 | 20 |
| $^{155,157}Gd$ enrichment [wt.%] | 70 | 70 | 70 | 50 | 70 |
| Content of natural gadolinia[wt.%] | - | 4 | - | 2 | - |
| $^{235}U$ in $UO_2$-$Gd_2O_3$ [wt.%] | 1.8 | 1.8 | 1.8 | 1.8 | 1.8 |

The control rods consist of four regulating bank groups (R4, R3, R2, R1) and seven shutdown bank groups (S1, S2, S3, S4, S5, S6, S7). Ag-In-Cd material is used for the regulating control rods to minimize the impact of control rod burnup, while $B_4C$ is used for the shutdown banks to enhance shutdown margin.

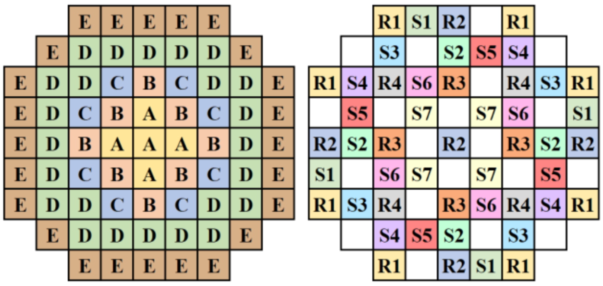


Fig. 4. Loading pattern (left) and control rod pattern (right)

## 3. Results

Fig. 5 shows the multiplication factor in the all rods out (ARO) depletion state and the critical positions of regulating banks R4 and R3 at each burnup. The multiplication factor achieved the target range, and the discharging burnup was 21.8 MWd/kg, satisfying the long-term operation goal of 30 months with 901 days.

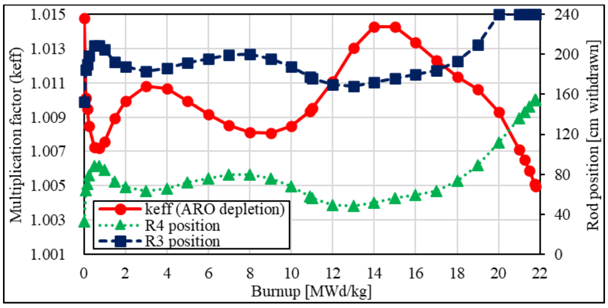


Fig. 5. $k_{eff}$ and critical control rod position from core depletion calculation

Fig. 6 presents both ASI values and $F_q$ values for the ARO depletion state and the rod operation state. In both cases, compared to the ARO depletion state, it can be seen that the power is concentrated in the bottom region due to the insertion of the control rod during rod operation. However, both ASI and $F_q$ values met the target values.

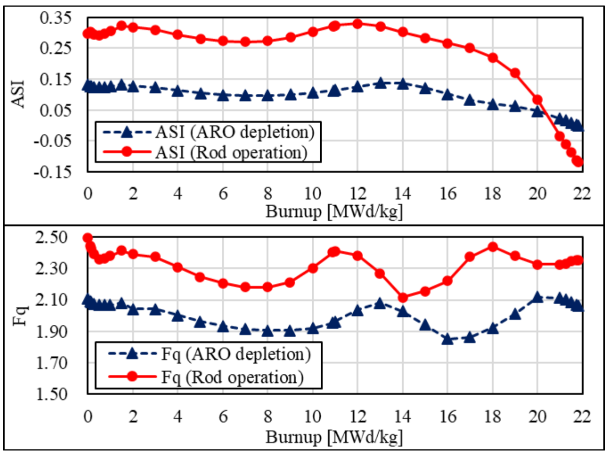


Fig. 6. Axial shape index (top) and 3D pin peaking factor (bottom)

To assess the impact of control rods, power distributions at BOC with maximum control rod insertion were analyzed. Fig. 7 illustrates that the central region of the core, which used fuel with lower enrichment, had intentionally lower fuel assembly power as expected. At BOC, the regulating bank R4 was inserted to 207.41 cm, while R3 was inserted to 87.41 cm. During control rod insertion, fuel assembly power decreased at both R4 and R3 positions. Specifically, R4, which was inserted 120 cm deeper than R3, showed a 31.3% decrease in power (from 1.15 to 0.79), whereas R3 showed only a 1.9% decrease (from 1.05 to 1.03). Fig. 8 shows that after control rod insertion, the axial power distribution shifts towards the bottom region.

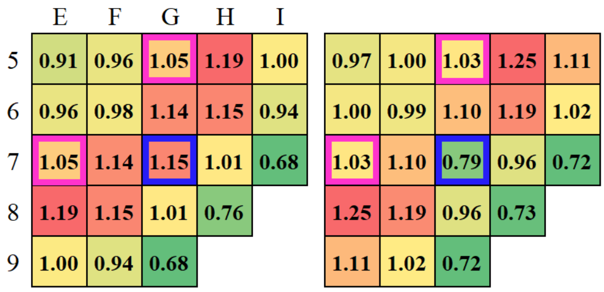


Fig. 7. Radial power distribution in the ARO depletion(left) and rod operation(right) states at BOC (blue box : R4 bank, pink box : R3 bank)

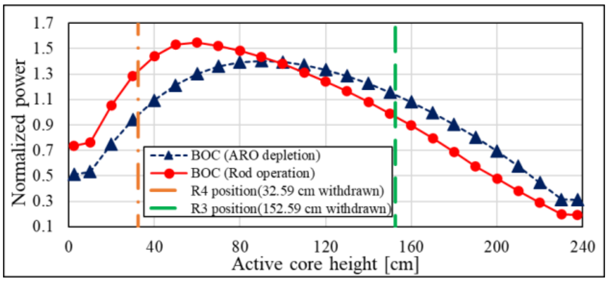


Fig. 8. Axial power distribution at BOC

Shutdown margin is important for ensuring the safety of the reactor. When the reactor transitions from hot full power (HFP) to hot zero power (HZP), a significant amount of positive reactivity is introduced into the core due to power defect and xenon burnout. Additionally, when transitioning to cold zero power (CZP), positive reactivity is further inserted due to the Doppler effect caused by changes in the temperature of the moderator and nuclear fuel. In reactors that operate without boron, such as those adopting SBF operation, the power defect and isothermal defect must be controlled solely by control rods. Failure to adequately manage this excess reactivity during the process can lead to accidents.

To enhance conservatism in shutdown margin calculations, it is assumed that the control rod with the highest worth is fully withdrawn from the core, thus having no impact on reactivity control. Fig. 9 shows the worth of each control rod, and the highest rod worth, considered as the stuck rod worth, was applied in line (2) of Table III. Shutdown margin calculations were conducted at BOC, MOC, and EOC, taking into account the effects of xenon. In all cases, the results exceeded the design limits as shown in Table III. Table IV presents the reactivity coefficients, including fuel temperature coefficient (FTC), moderator temperature coefficient (MTC), and isothermal temperature coefficient (ITC), as the reactor transitions from HFP to CZP. The coefficients are categorized into BOC, MOC, and EOC cases. The ITC, which combines MTC and FTC, was calculated with consistent treatment of fuel and moderator temperatures. The calculated ITC values were all negative and met the design limits, as shown in Table IV.

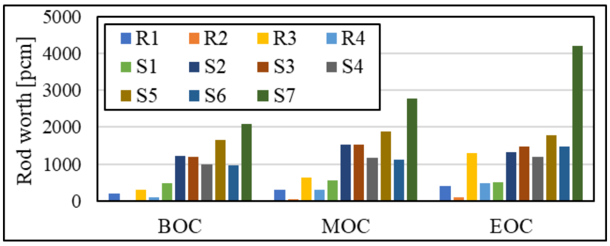


Fig. 9. Contorl rod worth by location of regulating bank and shutdown bank

Table III: Shutdown margin [pcm]

| State | BOC | MOC | EOC |
|---|---|---|---|
| All-rod-in worth (1) | 31,466 | 33,319 | 34,894 |
| Worth of worst stuck rod (2) | 2,080 | 2,764 | 4,194 |
| Uncertainty of rod worth (3) = (1) * 10% | 3,146 | 3,331 | 3,489 |
| Rod worth for criticality (4) = rod worth between ARO and criticality | 1,455 | 925 | 495 |
| Engineering error (5) | 100 | 100 | 100 |
| Real worth (6) = (1) – [(5) + (4) + (3) + (2)] | 24,685 | 26,199 | 26,616 |
| Power defect from HFP (equilibrium xenon) to HZP (no xenon) (7) | 3,796 | 4,013 | 4,510 |
| Isothermal defect (8) (HZP to CZP) | 7,599 | 4,833 | 5,356 |
| Engineering error (9) | 100 | 100 | 100 |
| Total defect (10) = (7) + (8) + (9) | 11,495 | 9,846 | 9,966 |
| Shutdown margin (11) = (6) – (10) | 13,190 | 17,253 | 16,650 |

Table IV: Reactivity coefficients [pcm/˚C]

| CASE | EFPD(day) | State | FTC | MTC | ITC |
|---|---|---|---|---|---|
| BOC | 0 | HFP | -2.62 | -56.68 | -59.60 |
| | | HZP | -3.02 | -57.01 | -60.03 |
| | | CZP | -3.24 | -12.31 | -15.56 |
| MOC | 451 | HFP | -2.86 | -53.06 | -54.99 |
| | | HZP | -3.47 | -52.62 | -56.09 |
| | | CZP | -3.57 | -7.43 | -11.00 |
| EOC | 901 | HFP | -3.17 | -54.99 | -58.16 |
| | | HZP | -3.80 | -53.82 | -57.62 |
| | | CZP | -3.85 | -3.52 | -7.37 |

## 5. Conclusions

This study showed that enriched gadolinia can enable SBF and long-cycle operation in SMRs without the need for new types of burnable absorbers. Enriched gadolinia improved thermal conductivity and controlled excess reactivity, while the $UO_2$-$Gd_2O_3$, which mixes enriched and low-content natural gadolinia, flattened the reactivity curve, enabling SBF and long-cycle operation.

The discharging burnup is 21.8 GWD/MTU, corresponding to a cycle length of 30 months. The $k_{eff}$ value is maintained between 1.005 and 1.015, while the $F_q$ value remains below 2.5. The ASI values range between -0.35 and +0.35. The ITC values are negative in all conditions, including HFP, HZP, and CZP. Additionally, the shutdown margin exceeds the design limit of 3,000 pcm in BOC, MOC, and EOC.

The reactor design, validated through simulations, met all safety and operational criteria, suggesting enriched gadolinia as a promising solution for future reactor designs. However, the feasibility of using enriched gadolinia depends on the availability of enrichment facilities and the associated costs. If these costs outweigh the economic benefits of extended cycle operation, its use may not be justified. Future research should focus on economic efficiency by placing enriched gadolinia in the reactor's central region, where power peaking and temperature rise are most critical, and using natural gadolinia in the outer regions.

## ACKNOWLEDGEMENT

This work was supported by the Innovative Small Modular Reactor Development Agency grant funded by the Korea Government (MSIT) (No. RS-2023-00258205).

## REFERENCES

[1] Y. G. Jo, H. C. Shin, Design Optimization of Cylindrical Burnable Absorber Inserted into Annular Fuel Pellets for Soluble-Boron-Free SMR, Nuclear Engineering and Technology, Vol. 54, pp. 1464-1470, 2022.

[2] J. S. Kim, T. S. Jung, J. I. Yoon, Reactor core design with practical gadolinia burnable absorbers for soluble boron-free operation in the innovative SMR, Nuclear Engineering and Technology, Vol. 56, pp. 3144-3154, 2024.

[3] J. C. Lee, S. Q. Zee, K. S. Kim, J. S. Song, A Study on the Nuclear Characteristics of Enriched Gadolinia Burnable Absorber Rods, KAERI/RR-2155/2000, 2001.

[4] J. S. Kim, B. H. Cho, S. G. Hong, Applicability Evaluation of Enriched Gadolinium as a Burnable Absorber in Assembly Level for Boron-Free i-SMR Core, Transactions of Korea Nuclear Society Spring Meeting, 2022.

[5] J. W. Choe, S. Y. Choi, P. Zhang, J. S. Park, W. K. Kim, H. C. Shin, H. S. Lee, J. E. Jung, D. J. Lee, "Verification and validation of STREAM/RAST-K for PWR analysis," Nuclear Engineering and Technology, Vol. 51, pp. 356-368, 2019.

[6] Advances in Small Modular Reactor Technology Developments, IAEA Advanced Reactors Information System (ARIS), 2020 Edition, 2020.